Current Topics in Biophysics 2010, 33 (suppl A), 27-31

COMPARISON OF EPR AND MAGNETIC SUSCEPTIBILITY MEASUREMENTS OF LITHIUM NIOBATE CRYSTALS WEAKLY DOPED WITH RARE-EARTH IONS

TOMASZ BODZIONY

Institute of Physics, West Pomeranian University of Technology, Szczecin, 70-310 Szczecin, Al. Piastow 17, Poland

Received June 12, 2010; accepted September 25, 2010; published online November 20, 2010.

Abstract: The results of the EPR and magnetic susceptibility measurements of weakly doped $LiNbO_3$: Er, Tm, $LiNbO_3$: Er, $LiNbO_3$: Yb, Pr and $LiNbO_3$: Yb single crystals are compared. Magnetic susceptibility measurements are an independent confirmation of the presence of the clustering sites of rare-earth RE^{3+} ions in weakly doped $LiNbO_3$ single crystal suggested previously on the basis of the optical and EPR measurements. It suggests that the distribution of the dopant ions in $LiNbO_3$ crystal weakly doped with RE^{3+} ions should be strongly inhomogeneous.

INTRODUCTION

Rare-earth (RE) doped lithium niobate, $LiNbO_3$ (LN), has excellent perspective of applications in integrated optics and actually has been utilized in many various technological applications (Properties of Lithium Niobate, 1989; Weis & Gaylord 1985). One should keep in mind that optical properties of any doped crystal are determined by the local symmetry of the optically active ions (Malovichko, Grachev, Kokanyan & Shirmer 1999; Dongfeng Xue & Xiangke He 2006; Dohnke, Trusch, Klimm & Hulliger 2004). LN crystal can be tuned to fit various experiment requirements. One of the methods applied to realize this tuning is doping. Rare-earth (RE) dopant ions: Er^{3+}, Yb^{3+} or Nd^{3+} are introduced to LN host as optically active impurities (Garcia-Sole, Bausa, Jaque, Montoya, Murrieta & Jaque, 1998; Bonardi, Magon, Vidoto, Terrile, Bausa, Montoya, Bravo, Martin & Lopez, 2001; Bravo & Martin, Lopez, 1999).

In this paper we focus on a comparison of EPR and magnetic susceptibility measurements of $LiNbO_3$ crystal weakly doped with ytterbium and erbium and co-doped with praseodymium and thulium. After experimental part, we will discuss the results of EPR measurements of magnetic measurements. We will discuss and summarize the results of these studies in the end,.

EXPERIMENTAL

$LiNbO_3$: Er^{3+} (0.2 wt. %), Tm^{3+} (0.3 wt. %) and $LiNbO_3$: Er (0.1 wt. %), $LiNbO_3$: Yb (0.8 wt. %), Pr (0.1 wt. %) and $LiNbO_3$: Yb (1.0 wt. %) single crystals were grown along the **c** - axis from the congruent melt by the Czochralski method in the Institute of Electronic Materials Technology, Warsaw, Poland. After mixing of adequate amounts of reagents the mixture was calcined at 1373 K for 6 h. The ingredients: Yb_2O_3 and Pr_2O_3 and Er_2O_3, Tm_2O_3 were added to the charge of the congruent melt with a Li/Nb ratio equal to 0.94, prior to synthesis at elevated temperatures. A more detailed description of the applied growth process was presented elsewhere (Pracka, Malinowski, Bajor, Surma, Gałązka, Swirkowicz & Mozdzonek, 1997).

Figure 1 shows the structure of the unit cell of the lithium niobate single crystal. The view of the cell is presented approximately along crystallographic ***c*** – axis. The LN structure is build of the oxygen atoms arranged in planar sheets, which form chains of trigonally distorted octahedra, adjoined by walls and spreading along the ***c*** – axis. The sequence of octahedra is: [Nb, vacancy, Li]. The ionic radius of Tm^{3+} ion is equal to 102 pm, Er^{3+} - 103 pm, Yb^{3+} – 100.8 pm, Tm^{3+} – 102 pm, whereas Li^{+} - 90 pm, Nb^{5+} – 78 pm, all in 6 - coordinated surroundings (www.webelements.com). Chains of octahedron connected by oxygen's ions are clearly visible in the Fig. 1. It means that 1/3 amount of the octahedral sites is empty. Consequently, lithium niobate lattice is flexible and Li^{+} sites (and/or Nb^{5+}) may be easy substituted by impurity ions, especially rare-earth ions. Additionally, assuming that Li^{+} (or Nb^{5+}) site is substituted by RE^{3+} ions, there are many (about 14 Li^{+} and Nb^{5+}) sites possible to substitute by other RE^{3+}ions in the closest neighborhood. These RE^{3+} may interact

with each other because distance between them is in the range form 3.1 Å to 3.9 Å.

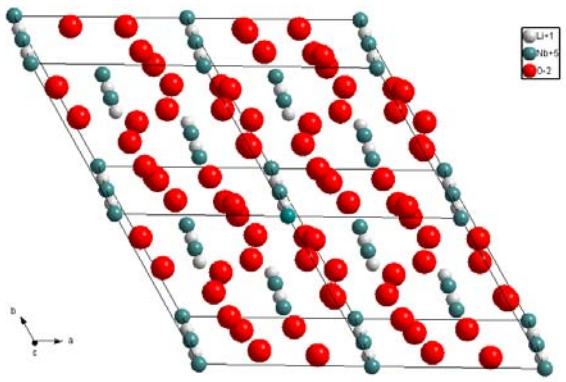

Fig.1. The structure of the $LiNbO_3$ crystal viewed approximately along c – axes.

EPR spectra were recorded using Bruker E 500 X-band spectrometer (ν~9.4 GHz) with 100 kHz field modulation equipped with Oxford flow cryostat for measurements at temperatures from liquid nitrogen temperature down to 4K. Magnetic susceptibility (MS) measurements were recorded using a Quantum Design magnetometer. First, the samples were cooled without magnetic field (zero field cooled, ZFC) and the measurements were carried out with temperature increasing from 4 K up to 40 K and applied magnetic field 200 Oe. In the next stage, the samples were cooled in magnetic field 200 Oe (field cooled, FC) down to 4.5 K and the measurements were carried out with temperature increasing up to 40 K in the same magnetic field. The measurements were performed in the Institute of Nanotechnology, Karlsruhe, Germany.

EPR MEASUREMETS

We would like to show only these ERP results, which we can compare with magnetic susceptibility measurements, especially on the temperature dependency of the total intensity of the EPR spectra. The total intensity of the EPR lines is obtained by double integration of the EPR spectrum.

Figure 2 shows the temperature dependence of the total intensity (solid circles, the left axis), the inverse of the total intensity (empty circles, the right axis) of the main EPR line of LN: Er (0.1 wt.%) single crystal (Bodziony & Kaczmarek, 2007). Figure 2 also presents the temperature dependence of the total intensity (solid squares, the left axis), the inverse total intensity (empty squares, the right axis) of the main EPR line of LN: Er (0.2 wt.%), Tm (0.3 wt.%) single crystal (Bodziony & Kaczmarek, 2009). One should noticed that the total intensity for both crystals are presented in different scale. The total intensity of the EPR lines is much greater in co-doped sample than in the doped only with Er sample, even taking into account ratio of the input concentrations of impurities (see Fig. 2). The temperature dependency of the total intensity of the LN: Er, Tm revels characteristic two-peak pattern. The total intensity reaches a maximum and decreases at lower temperatures in the case of LN: Er (Bodziony & Kaczmarek, 2007, Bodziony & Kaczmarek. 2009).

The inverse intensity at low temperature region fulfils the Curie–Weiss law in low temperature region below ~20 K and ~35 K for LN: Er and LN: Er, Tm single crystals, respectively (see Fig. 2, empty circles and squares). The positive sign of Curie constant suggests ferromagnetic interactions arise in the system of Er^{3+} ions in both LN: Er and LN: Er, Tm single crystals.

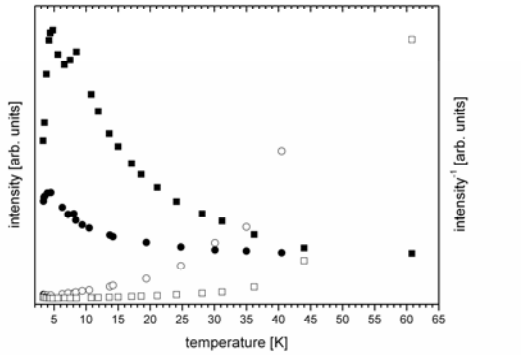

Fig.2. The temperature dependence of the total intensity of the EPR lines (the left axis, solid squares and solid circles) and the inverse of the total intensity (the right axis, empty squares and empty circles) for $LiNbO_3$: Er (0.2 wt. %), Tm (0.3 wt. %) (solid, empty squares) and $LiNbO_3$: Er (1.0 wt. %) (solid, empty circles) single crystals.

Figure 3 shows the analogous dependencies for $LiNbO_3$: Yb (0.8 wt. %), Pr (0.1 wt. %) and $LiNbO_3$: Yb (1.0 wt. %) samples. The total intensity of the EPR spectra for $LiNbO_3$: Yb (0.8 wt. %), Pr (0.1 wt. %) and $LiNbO_3$: Yb (1.0 wt. %) single crystals are marked by solid squares and solid circles, respectively (Bodziony, Kaczmarek & Hanuza, 2008a; Bodziony, Kaczmarek & Rudowicz, 2008b). The inverse of the total intensity (the right axis) are marked by empty squares and empty circles for above samples, respectively. Similarly, the scales are different for both samples. One can see again that the total intensity of the EPR spectrum is much greater in co-doped sample (LN: Yb, Pr) than in the doped only LN: Yb sample, even taking into account differences in the input concentration of impurities (see

Fig. 3).

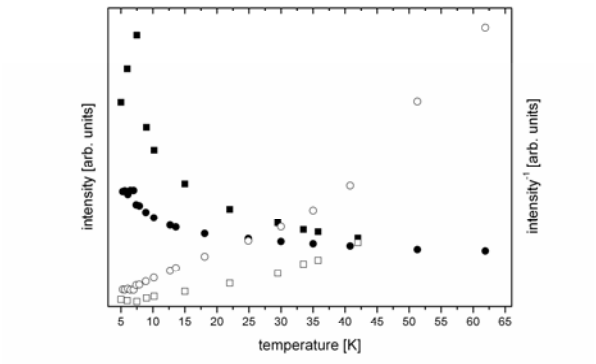

Fig.3. The temperature dependence of the total intensity of the EPR lines (the left axis, solid squares and solid circles) and the inverse of the total intensity (the right axis, empty squares and empty circles) for $LiNbO_3$: Yb (0.8 wt. %), Pr (0.1 wt. %) and $LiNbO_3$: Yb (1.0 wt. %) single crystals solid, empty squares and solid, empty circles, respectively.

The EPR line intensity fulfils Curie–Weiss law in both samples in the low temperature region (below ~35 K, see Fig. 3, empty circles and squares). The estimated Curie constant has the negative value in case $LiNbO_3$:Yb, which suggests antiferromagnetic interaction between ytterbium ions but positive value, which indicates ferromagnetic interaction in the case codoped $LiNbO_3$:Yb, Pr samples. The presence of co-dopant (praseodymium) significantly changes properties of $LiNbO_3$:Yb single crystal (Bodziony, Kaczmarek & Hanuza, 2008a; Bodziony, Kaczmarek & Rudowicz, 2008b).

MACNETIC SUSCEPTIBILITY MEASUREMETS

Figure 4 shows the temperature dependence of the magnetic susceptibility $\chi(T)$ (the left axis) and the inverse of the magnetic susceptibility $1/\chi(T)$ (the right axis) for $LiNbO_3$: Yb (0.8 wt. %), Pr (0.1 wt. %) single crystal in ZFC and FC regimes (Bodziony, Kaczmarek, & Kruk, 2010a). ZFC and FC points are marked by squares or circles, respectively, whereas the magnetic susceptibility and the inverse of the magnetic susceptibility $1/\chi(T)$ are distinguish by solid and empty marks (see Fig. 4). ZFC and FC points are nearly superimposed onto each other. One can see from Fig. 4 that the inverse susceptibility increases linearly with increasing temperature (see Fig.4, empty squares and circles). In fact, the dependence of magnetic susceptibility versus temperature fulfills the Curie-Weiss law. The estimated Curie parameter has negative value and indicates the presence of antiferromagnetic interactions in weakly doped $LiNbO_3$:Yb, Pr single crystal (Bodziony *et al.,* 2010a).

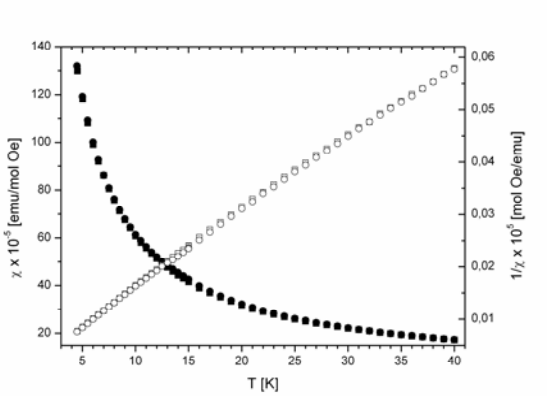

Fig. 4. The temperature dependence of the magnetic susceptibility $\chi(T)$ (the left axis, solid marks) and the inverse of the magnetic susceptibility $1/\chi(T)$ (the right axis, empty marks) for $LiNbO_3$: Yb (0.8 wt. %), Pr (0.1 wt. %) single crystal in ZFC and FC regimes (squares and circles, respectively).

Figure 5 presents the temperature dependence of the magnetic susceptibility $\chi(T)$ (the left axis) and the inverse of the magnetic susceptibility $1/\chi(T)$ (the right axis) for $LiNbO_3$: Er (0.2 wt. %), Tm (0.3 wt. %) single crystal in ZFC and FC regimes (Bodziony, Kaczmarek & Kruk, 2010b). The inset shows the high temperature dependence of the magnetic susceptibility.

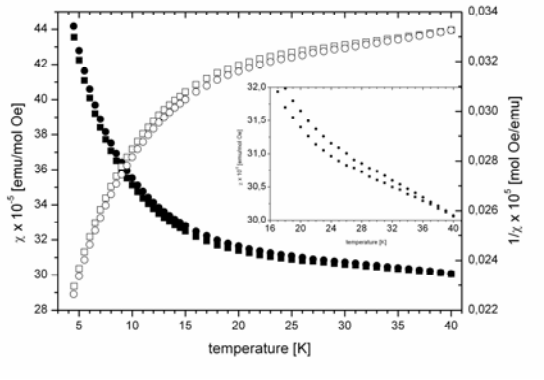

Fig. 5. The temperature dependence of the magnetic susceptibility $\chi(T)$ (the left axis, solid marks) and the inverse of the magnetic susceptibility $1/\chi(T)$ (the right axis, empty marks) for $LiNbO_3$: Er (0.2 wt. %), Tm (0.3 wt. %) single crystal in ZFC and FC regimes (squares and circles, respectively); the inset shows the high temperature dependence of the magnetic susceptibility.

Marks used in Fig. 5 have the same meaning as in Fig.4. The behavior of magnetic ions is much more complicated in the case of LN: Er, Tm crystal than LN:

Yb, Pr (see Fig. 4 and 5). The inverse magnetic susceptibility increase approximately linearly in low (below ~16 K) and high (above ~20 K) temperature range, for example. These two regions are connected by a gentle arc. Magnetic susceptibility points fulfills the Curie-Weiss law in low and high temperature region (see Fig.4). The Curie-Weiss law suggests the presence of the interacting systems of Er, Tm, and mixed Er/Tm ions. (Bodziony *et al.,* 2010b). Magnetic susceptibility measurements of the $LiNbO_3$: Er (0.2 wt. %), Tm (0.3 wt. %) sample is determined by the presence of two types of magnetic ions: Er^{3+} and Tm^{3+} in the host.

DISCUSSION AND CONCLUSIONS

Comparison of the results of EPR and MS measurements shows that both methods lead to similar conclusions. EPR and MS measurements confirm the presence of magnetically interacting RE ions in LN host. Crystallographic analysis confirm this possibility (see Fig. 1). It means that these ions must be close together in the unit cell taking into account low concentration of impurities. We suggested previously a possibility of presence RE^{3+}-RE^{3+} pair of ions (Bodziony *et al.,* 2008a). The presence of Yb^{3+} pairs within the $LiNbO_3$ matrix was also indicated by others (Montoya, Espeso & Bausa, 2000). However, there are many possible sites in the closets neighborhood of the RE_{Li} (or RE_{Nb}) ion (see Fig. 1). The compensation mechanism may enforce substitute some of them by dopant ions. In result we will obtain a clusters of RE ions, even in the case of weak input concentration of impurities.

Very important role is played by the second admixture or co-dopant (Torchia, Martinez Matos, Vaveliuk & Tocho 2003). Diaz-Caro *et al.,* investigated the optical spectra of co-doped $LiNbO_3$:Cr:MgO crystals (Diaz-Caro, Garcia-Sole, Martinez, Henderson, Jaque & Han, 1998). They concluded that the concentration of the MgO above 4 % (co-dopant) indicate a transfer of Cr^{3+} ions from Li^+ to Nb^{5+} sites. We have a case of lithium niobate crystal weakly doped with rare-earth ions. Nevertheless, it seems that the coodpant may play analogous role as MgO or ZnO compounds. The redistribution effect of the main dopant (Er^{3+} or Yb^{3+}) between Li^+ and Nb^{5+} sites may be caused by the presence of co-dopant (Tm^{3+} or Pr^{3+}) ions. RE^{3+} ions occupying neighboring positions in the cell may interact magnetically with each other (see Fig. 1) and further these interactions we may record in EPR or MS measurements.

Our results suggest that RE ions form clusters in LN hosts despite of weakly input concentration of impurities. Consequently, the distribution of RE ions in congruent LN should be strongly inhomogeneous. These results may be important in practical applications of doped lithium niobate crystals, for example in optics. We can affect the optical properties of Yb or Er by adding an appropriate dopant in the right concentration. The study of these relationships is the aim of further work.

REFERENCES

Bodziony T. & Kaczmarek S. M. (2007). EPR and optical measurements of weakly doped $LiNbO_3$: Er, *Physica B*, **400,** 99 – 105.

Bodziony T., Kaczmarek S. M. & Rudowicz C. (2008a).Temperature dependence of the EPR lines in weakly doped $LiNbO_3$: Yb - possible evidence of Yb^{3+} ion pairs formation, *Physica B*, **403**, 207 – 218.

Bodziony T., Kaczmarek S. M. & Hanuza J. (2008b). EPR and optical studies of $LiNbO_3$:Yb and $LiNbO_3$:Yb, Pr single crystals, *Journal of Alloys and Compounds*, Vol. 451/1-2, 240 – 247.

Bodziony T. & Kaczmarek S. M. (2009). Temperature dependence of the EPR spectra and optical measurements of LiNbO3: Er, Tm single crystal, *Journal of Alloys and Compounds*, **468,** 581 – 585.

Bodziony T., Kaczmarek S. M. & Kruk R. (2010a). Magnetic properties of $LiNbO_3$ single crystals weakly doped by Yb and/or codoped by Pr, *Rev.Adv.Mater.Sci*. **23**, 1-7.

Bodziony T., Kaczmarek S. M. & Kruk R. (2010b). Low temperature magnetic measurements of $LiNbO_3$ single crystal weakly doped with Er and codoped with Tm ions, *Physica B*, not yet published.

Bonardi C., Magon C. J., Vidoto E. A., Terrile M. C., Bausa L. E., Montoya E., Bravo D., Martin A. & Lopez F. L (2001). EPR spectroscopy of Yb^{3+} in $LiNbO_3$ and Mg: $LiNbO_3$, *Journal of Alloys and Compounds*, **323—324,** 340-343.

Bravo D., Martin A. & Lopez F. J. (1999). A new centre of Er^{3+} in MgO or ZnO co-doped $LiNbO_3$ single crystals, *Solid State Commun.*, **112**, 541- 544.

Diaz-Caro J., Garcia-Sole J., Martinez J.L, Henderson B., Jaque F. & Han T.P.J (1998). Redistribution of Cr^{3+} defect centres in $LiNbO_3$ crystals: the MgO effect, *Optical materials*, **10**, 69-77.

Dohnke I., Trusch B., Klimm D. & Hulliger J. (2004). A study of influence of ytterbium and impurities on lattice parameters and phase transition temperature of Czochralski-grown $LiNbO_3$, **65**, 1297-1305

Xue D. & He X. (2006). Dopant occupancy and structural stability of doped lithium niobate crystals, *Phys. Rev. B*, **73,** 064113-1 – 064113-7.

Garcia-Sole J., Bausa L.E., Jaque D., Montoya E., Murrieta H. & Jaque F. (1998). Rare earth and transition metal ion centers in $LiNbO_3$, *Spectrochimica Acta Part A*, **54**, 1571-1581.

Malovichko G., Grachev V., Kokanyan V. & Shirmer O. (1999). Axial and lo-symmetry centers of trivalent impurities in lithium niobate: Chromium in congruent and stoichiometric crystals, *Phys. Rev. B*, **59,** 9113-9125.

Montoya E., Espeso O. & Bausa L.E. (2000). Cooperative luminescence in Yb^{3+} : $LiNbO_3$, *Journal of Luminescence*, **87-89**, 1036-1038 .

Pracka I., Malinowski M., Bajor A.L., Surma B., Gałązka Z., Swirkowicz M. & Mozdzonek M. (1997). *Proc. SPIE* vol. **3178** 295.

Properties of Lithium Niobate (1989). EMIS Datareviews Series No. 5, Inspec.

Torchia G.A., Martinez Matos O., Vaveliuk P. & Tocho J.O. (2003). Influence of electron-lattice coupling for Cr^{3+} ions in Nb^{5+} site into congruent co-doped $LiNbO_3$: Cr^{3+}: ZnO crystals, *Solid State Commun.*, **127**, 535-539.

Weis R.S & Gaylord T.K. (1985). Lithium niobate: Summary of physical Properties and Crystal Structure, *Appl. Phys. A.*, **37**, 191-203.